HHS Public Access

Author manuscript

Nat Neurosci. Author manuscript; available in PMC 2017 March 01.

Published in final edited form as:

Nat Neurosci. 2016 September ; 19(9): 1250–1255. doi:10.1038/nn.4354.

Connectivity precedes function in the development of the visual word form area

Z.M. Saygin[1,2], **D.E. Osher**[3], **E.S. Norton**[4], **D.A. Youssoufian**[5], **S.D. Beach**[1,2], **J. Feather**[6], **N. Gaab**[7], **J.D.E. Gabrieli**[1,2], and **N. Kanwisher**[1,2]

[1]Department of Brain and Cognitive Sciences, Massachusetts Institute of Technology, Cambridge, Massachusetts, USA.

[2]McGovern Institute for Brain Research, Massachusetts Institute of Technology, Cambridge, Massachusetts, USA.

[3]Department of Psychological and Brain Sciences, Boston University, Boston, Massachusetts, USA

[4]Department of Communication Sciences and Disorders, Northwestern University, Evanston, Illinois, USA

[5]Department of Biological Sciences, Barnard College, Columbia University, New York, New York, USA

[6]Department of Bioengineering, University of California, Berkeley, California, USA

[7]Boston Children's Hospital, Boston, Massachusetts, USA

Abstract

What determines the cortical location where a given functionally specific region will arise in development? Here we test the hypothesis that functionally specific regions develop in their characteristic locations because of pre-existing differences in the extrinsic connectivity of that region to the rest of the brain. We exploit the Visual Word Form Area (VWFA) as a test case, scanning children with diffusion and functional imaging at age five, before they learned to read, and at age 8, after they learned to read. We find the VWFA develops functionally in this interval and that its location in a particular child at age 8 can be predicted from that child's connectivity fingerprints (but not functional responses) at age 5. These results suggest that early connectivity instructs the functional development of the VWFA, possibly reflecting a general mechanism of cortical development.

Correspondence should be addressed to Z.M.S. (zsaygin@mit.edu).

AUTHOR CONTRIBUTIONS

Z.M.S., D.E.O., and N.K designed the experiments. Z.M.S., E.S.N, D.A.Y., S.D.B., N.G., J.D.E.G. and N.K. conducted the experiments or supplied data. Z.M.S., D.E.O., D.A.Y., and J.F. analyzed the data. Z.M.S., D.E.O., and N.K. wrote the manuscript.

COMPETING FINANCIAL INTERESTS

The authors declare no competing financial interests.

A Supplementary Methods Checklist is available.

INTRODUCTION

The last two decades of neuroimaging research have revealed the functional organization of the human brain in unprecedented detail. Dozens of cortical regions have been identified, each with a distinctive functional profile, and each found in approximately the same anatomical location in virtually every normal adult. How does this systematic functional organization arise in development? Here we ask specifically how a particular cortical location becomes earmarked as the future site where a particular functionally specific region will develop.

A clue comes from previous findings in adults showing a close and fine-grained relationship between the functional response profile of each voxel in a region of cortex, and the extrinsic connectivity of that voxel to the rest of the brain, measured with diffusion tractography in the same subject[1,2]. This tight relationship between function and connectivity across the cortex suggests a developmental hypothesis: patterns of extrinsic connectivity (or "connectivity fingerprints") may arise early in development, instructing subsequent functional development[3,4]. Prior evidence for this hypothesis comes from classic studies in ferrets showing that if retinal input is rerouted to medial geniculate nucleus (MGN) and subsequently primary auditory cortex (A1), A1 takes on many functional properties of V1[5,6,7,8,9]. However, it remains unclear whether similar mechanisms underlie the development of nonprimary cortical regions whose main input is not from the thalamus but from other cortical regions.

Here we test the Connectivity hypothesis for the case of the visual word form area (VWFA)[10,11,12,13,14], a ventrolateral region that responds much more strongly to visually presented words or letter strings than to other visually-similar stimuli, including digit strings, faces, and words written in an unfamiliar orthography (e.g. Chinese or Hebrew for English speakers)[15]. Crucially, these patterns develop with reading experience and ability, and are only present in readers[11]. According to the Connectivity hypothesis, the eventual cortical site of the VWFA should be predicted by its earlier-developing extrinsic connections to other brain regions, i.e., pre-reading connectivity patterns should predict the eventual location of the VWFA after a child learns to read. Alternative (but not mutually exclusive) hypotheses are that the location of the VWFA is determined by the intrinsic molecular or circuit properties of that piece of cortex, or by pre-existing featural[16–19] or retinotopic selectivities that predispose this region to develop orthographic selectivity. To test the Connectivity hypothesis, we scanned children longitudinally both before and after they learned to read, and tested whether the VWFA develops in this interval, and whether the specific location where the VWFA develops is predictable from the connectivity fingerprint of that same region before children learn to read.

RESULTS

Functional Selectivity of VWFA and lFFA

We defined a word-selective VWFA in each individual's age 8 data as any voxels that respond more strongly to words than line-drawings of objects (at $p<0.005$ uncorrected in half the functional runs) within a VWFA constraint region (Supplementary Figure 1; also see

Online Methods). We defined face-selective cortex similarly (i.e. any voxels within a left FFA constraint region that respond higher to line-drawings of faces than to line-drawings of objects, at $p<0.005$ in half the functional runs).

We found both a VWFA and left fusiform face area (lFFA) in 29/31 (94%) of the children we scanned at age 8. Fourteen of these children could not yet read at age 5, and had an fMRI scan at age 5, so our main fMRI analyses focused on this cohort. At age 8, all of these children could read, and had both a VWFA and lFFA (see **Online Methods** for further details). We extracted the magnitude of response (percent signal change from a no-stimulus baseline) from these regions for each of the stimulus categories in fMRI runs independent of those used to define the regions at age 8 (see Figure 1). The VWFA and lFFA were clearly distinct in their responses to the stimulus categories (2-way repeated measures ANOVA of ROI × condition: $F_{3,78} = 24.56$; $P = 2.72 \times 10^{-11}$). The VWFA responded more strongly to words than it did to other visually similar stimuli, including line-drawings of faces, scrambled words, and line-drawings of objects (repeated measures ANOVA by condition: $F_{3,39} = 10.96$, $P = 2.34 \times 10^{-5}$; Figure 1). The left FFA responded more strongly to line-drawings of faces than to objects, words, and scrambled words ($F_{3,39} = 34.30$, $P = 5.03 \times 10^{-11}$; Figure 1).

No Evidence for Early Functional Differentiation of VWFA

We then measured the response profiles of these same fROIs at age 5, before these children learned to read, by registering each child's age 8 VWFA and lFFA to their own fMRI data at age 5 (see **Online Methods**). We found that at pre-reading, VWFA was not selective to orthography: the VWFA did not show any selectivity to letters over faces or false font letters (repeated measures ANOVA by condition: $F_{2,26} = 1.67$, $P = 0.21$; Figure 1) whereas the lFFA already showed strong selectivity to faces over letters or false fonts even at age 5 ($F_{2,26} = 14.02$, $P = 7.41 \times 10^{-5}$; Figure 1). Additional analyses (see **Online Methods**) show that the VWFA in adults responds similarly to words and individual letters, so the use of individual letters in the 5-year-olds should be a good measure of the selectivity of this region.

Further, to test whether our fMRI methods at age 5 (stimuli and scanning parameters) were sufficient to detect a VWFA at age 5 if it were there, we also analyzed a small group of children (n = 8) who could read at age 5 and who were scanned again at age 8 ("readers"). We performed three different types of analyses in these children and compared them to the pre-readers. First, we found that the VWFA (defined at age 8) does show significant selectivity to letters at age 5 in children who could already read at that age. This analysis shows that we can detect word/letter selectivity when it is present at age 5, with the same contrasts and scanning parameters used in the main cohort of children who could not read at age 5 (Supplementary Figure 2). Second, to test the hypothesis that letter selectivity may have been present at age 5 but in a different location from the same child's VWFA at age 8, we performed a "binned analysis" that did not rely on localization in the 8-year-old data. We again found that children who could not read at age 5 did not show selectivity to letters vs. false fonts or faces (Figure 2), but children who *could* read at age 5 showed selectivity to both letters vs. false fonts and letters vs. faces (Supplementary Figure 3). Both groups showed selectivity for words at age 8 (when they could all read). This analysis further

bolsters the conclusion that there is no word/letter selectivity at age 5 in children who could not read. Third, using an MVPA analysis (i.e. correlation of voxelwise signal between and across stimulus conditions[20]), we found that classification accuracy was at chance for discriminating letters (from faces or false fonts) in the 5-year-old data of children who could not read at age 5, when tested in that child's 8-year-old VWFA fROI. In contrast, classification performance was significantly above chance for letters (vs. false fonts or faces) in children who could already read at age 5 (Supplementary Figure 4). Note that the VWFA in the early readers was defined using only age 8 data; the age 5 data only had three stimulus conditions and therefore could not be used to define the contrast of Words > Objects (which is what is used in the rest of the paper and used previously to define the VWFA e.g. [15]). However, the three conditions at age 5 are sufficient to show a letter-preferring region only in the readers at that age. Altogether, these results show that the region that will later become the VWFA cannot discriminate letters from non-letter stimuli before these children can read. The characteristic functional selectivity of the VWFA is found only in children who can read.

These data also show that while the VWFA is not selective for orthography in children who cannot read, the lFFA is already selective for faces at age 5. Note that we also find no selectivity for faces in the VWFA at age 5 in these children (as reported above) and that there is no change in the VWFA's response to faces from age 5 to age 8 ($P = 0.927$; $T(13) = 0.094$). These data suggest that early feature selectivity in the VWFA (at least for the stimuli that we have tested here) does not determine its later functional profile. Other evidence against this hypothesis comes from an analysis of left posterior fusiform sulcus (lPFS), a nearby region that responds selectively to shape[17] (see Figure 1). The response profile of the VWFA and adjacent lPFS (defined at age 8 and registered to the 5-year-old data) were not significantly different from each other at age 5 (fROI × condition repeated measure ANOVA: $F_{2,52} = 1.64$, $P = 0.20$), but were at age 8 (for the same subjects and same three conditions as age 5, i.e. no objects condition; fROI × condition ANOVA: $F_{2,52} = 5.59$, $P = 7.06 \times 10^{-8}$). These data provide no evidence that the cortical tissue that will become the VWFA is earmarked for that function by a distinctive functional response before word selectivity develops. They also argue against the hypotheses that the VWFA takes over cortical regions that were previously selective for object shape or faces[16,18,19,21].

Testing the Connectivity Hypothesis for Word-Selectivity

We next tested the hypothesis that pre-existing connectivity determines the location of the VWFA, by asking whether each child's voxel-by-voxel connectivity data at age 5 can predict the location of the same child's word-selectivity at age 8. Eleven children had a useable DWI (diffusion-weighted scan) at age 5, so our longitudinal DWI analyses focused on this cohort (the fMRI selectivity results remained the same as above even in these eleven children; see Supplementary Materials). We focused on the left occipitotemporal anatomical parcel (i.e. combined Freesurfer parcel of fusiform and inferior temporal cortex; lOTC parcel) and trained a model to learn the relationship between the connectivity of each voxel in this region at age 5 and fMRI activation patterns at age 8 in the same individuals, and tested the model on new children (in a leave-one-out manner; see **Online Methods**), as described previously by our group[1,2] and adapted subsequently by other groups[22]. We found

that early connectivity was able to predict the later spatial profile of word-selectivity in these children (Figure 3); the correlation across voxels in the left occipitotemporal parcel between the actual fMRI t-statistic values for Words > Objects at age 8 and the predicted fMRI values from connectivity was 0.47 ± 0.036 (mean Fisher z across all subjects). These predictions were significantly better than chance for each subject individually at $P < 0.05$ (based on random permutations exact tests per subject; P=0.014 for one subject, P=0 for all other subjects).

To better assess the strength of these DWI predictions and how well they captured individual differences in spatial patterns of functional selectivity, we compared the DWI predictions to predictions generated from the fMRI data of other subjects at age 8. First, we generated group average predictions; we performed a random effects analysis on the Words > Objects contrast data from all but one subject in template space, and mapped these values to the native space data of the subject we left out. This procedure generated voxelwise neural responses for word-selectivity in each individual based on aggregate responses from all other participants. We found that the correlations between actual and predicted word-selectivity from this group average analysis were much lower (Figure 4; mean Fisher z = 0.26 ± 0.042) than the predictions from the same individual's connectivity (paired t-test of Fisher z correlations of DWI predictions vs. group-average predictions: $T_{10} = 5.63$; $P = 2.20 \times 10^{-4}$).

Next, we compared the DWI predictions to predictions generated from each other subject's fMRI data individually. We registered each child's fMRI data from age 8 to each other child's DWI data at age 5, and generated voxelwise predictions for each subject based on every other's child's data. These predictions were less accurate than the predictions of an individual's own fMRI data (Figure 4; mean Fisher z: 0.25 ± 0.027; $T_{10} = 6.85$; $P = 4.48 \times 10^{-5}$). Thus, each individual's connectivity data at age 5 better predicted the same child's functional activation pattern at age 8 than did another child's fMRI data. These results indicate that the prediction of functional activation patterns from connectivity at age 5 is spatially precise enough to predict individual differences in functional activation patterns.

Random permutations represent the lowest bar that the DWI predictions should surpass in order to be considered accurate. To get an idea of the *best* possible predictive correlation values, we then asked how well half of each individual's own fMRI data at age 8 would predict the other half of fMRI data in the same subject (i.e. split-half reliability of age 8 fMRI data). The predictions reported above were generated from all of the fMRI data; for direct comparability with the same amount of data in each case, we next generated predictions from DWI connectivity from *half* the fMRI data (z = 0.46 ± 0.041) and compared these predictions to predictions from the split-half fMRI data (z = 0.69 ± 0.086; Figure 3c). As expected, the split-half correlations outperformed predictions from age-5 DWI ($T_{10} = 3.87$; $P = 3.09 \times 10^{-3}$). Children with higher correlation values between actual vs. predicted also had higher scan-to-scan reliability ($R = 0.77$; $P = 5.63 \times 10^{-3}$). After normalizing for scan-to-scan reliability (which included the same amount of fMRI data as the DWI predictions), we found that connectivity predicted about 70% of the reliable variance in Words > Objects responses ($R^2 = 0.69 \pm 0.015$).

We also compared the longitudinal DWI predictions of word-selectivity to predictions of face-selectivity, generated in exactly the same manner (age 5 DWI to predict age 8 fMRI). Predictions of word-selectivity were comparable to predictions of face-selectivity (z = 0.47 ± 0.036 vs. 0.43 ± 0.061 respectively; t-test of correlation values for word vs. face-selectivity predictions: $T_{10} = 0.50$; P = 0.63). Using DWI data collected at age 8, we also compared the longitudinal predictions to the within time-point predictions. We generated predictions of age 8 word-selectivity from age 8 DWI data and found no significant difference between the across-time predictions vs. within-time predictions ($T_{10} = 1.42$; P = 0.19).

We then asked how well connectivity predicted the VWFA fROI in particular i.e. not the full gradient of Words > Objects responses within the large anatomical occipitotemporal parcel, but the thresholded and positive (i.e. word-selective) responses within the VWFA constraint region (i.e., the smaller region that contains the VWFA fROI in most subjects, or "GSS parcel"; see **Online Methods**). For each subject, we created a VWFA fROI from the DWI-predicted activations and compared it to the same subject's actual functionally-defined VWFA. We found that the predicted VWFA overlapped with the actual VWFA by 64% (overlap coefficient = 0.635 ± 0.058; ranging from 0.84 ± 0.03 for the most lenient thresholds to 0.45 ± 0.09 for highest thresholds; the overlap coefficient is defined as the size of intersection divided by the smaller of the two sets, and equals 1 if an fROI is a subset of the other). We also looked at how far away the predicted VWFA was from the actual VWFA. We used the modified Hausdorff metric, which describes the mean distance of all points in the predicted fROI from the closest points in the actual fROI. The VWFA predicted from DWI was on average 0.65 ± 0.12 voxels (1.3 ± 0.4 mm) away from the actual VWFA (ranging from 0.49 ± 0.11 voxels or 0.98 ± 0.22 mm for the most lenient thresholds to 0.98 ± 0.28 or 1.96 ± 0.56 mm for highest thresholds). That is, the estimated VWFA location from the DWI-predicted data was less than one voxel, or 1.3mm on average, away from an individual's true VWFA. As a comparison, the VWFA fROI generated from the split-half fMRI data (i.e. best possible overlap metric) had an overlap coefficient of 0.865 ± 0.014 and Hausdorff metric of 0.26 ± 0.049 voxels.

These results strongly suggest that the VWFA already has distinct connectivity patterns even at age 5 when a child cannot yet read and when that same cortical region shows no orthographic selectivity. Our final analyses asked what these distinct connectivity patterns were; specifically, we defined the VWFA, and two adjacent fROIs (lFFA and lPFS) and compared the connectivity patterns of each of these fROIs to the rest of the brain. We ran tractography on the 5-year-old data from each fROI (VWFA, lFFA, lPFS, defined on the 8-year-old data and registered to the 5-year-old data) to every other brain region (defined anatomically from Freesurfer sulcal/gyral segmentation). We first performed an ANOVA of seed (VWFA, lFFA, or lPFS) × target. We found a significant main effect of seed ($F_{2,2430} = 18.54$, $P = 1.02 \times 10^{-8}$) and significant seed × target interaction ($F_{160,\ 2430} = 3.39$, $P = 2.20 \times 10^{-37}$), indicating significant differences in the connectivity patterns for different fROIs. To further explore the differences between VWFA and each of lFFA and lPFS, we subsequently ran a 2-way ANOVA of VWFA vs. lFFA × target, and VWFA vs. lPFS × target separately. The VWFA was significantly more connected in general than the lFFA (significant main

effect; $F_{1,1620} = 30.01$, $P = 4.97 \times 10^{-8}$); these were not global differences in connectivity but were rather due to differences between the two fROIs in their connectivity to certain target regions (interaction effect $F_{80,1620} = 1.92$, $P = 3.64 \times 10^{-6}$). Specifically, the VWFA was more strongly connected than lFFA was to left-lateralized temporal and frontal parcels (middle temporal: $P = 3.41 \times 10^{-4}$; $T(10) = 5.31$; superior temporal: $P = 1.44 \times 10^{-2}$; $T(10) = 2.95$; transverse temporal: $P = 4.29 \times 10^{-2}$; $T(10) = 2.32$; lateral orbitofrontal: $P = 4.30 \times 10^{-2}$; $T(10) = 2.32$) which may correspond with putative language regions (in line with recent tractography studies in adults[23,24]) as well as the left precentral gyrus ($P = 4.28 \times 10^{-2}$; $T(10) = 2.32$), inferior parietal ($P = 2.93 \times 10^{-2}$; $T(10) = 2.54$), entorhinal cortex ($P = 3.18 \times 10^{-2}$; $T(10) = 2.49$), ventral diencephalon ($P = 4.49 \times 10^{-2}$; $T(10) = 2.29$), and putamen ($P = 4.56 \times 10^{-2}$; $T(10) = 2.28$; cortical targets displayed in Figure 5). We also found differences between the VWFA and lPFS in their connectivity to specific target regions (ns main effect: $F_{1,1620} = 1.70$, $P = 0.19$; significant interaction effect: $F_{80,1620} = 2.82$, $P = 1.67 \times 10^{-14}$). The VWFA was more connected than lPFS with the left middle temporal gyrus ($P = 2.90 \times 10^{-3}$; $T(10) = 3.91$) while the lPFS was more connected than the VWFA with only the left lingual gyrus ($P = 3.76 \times 10^{-4}$; $T(10) = –5.25$; Figure 5). The VWFA's connectivity with the rest of the brain at age 5 is therefore distinct from the connectivity patterns of both the adjacent lPFS and lFFA, despite a lack of functional differentiation at this age.

In sum, these results show that the precise location of the VWFA is accurately predicted from the connectivity of this region even before the functional specialization for orthography in VWFA exists. fMRI selectivity to words does not exist before a child learns to read, but there are already differences in the connectivity fingerprints of voxels that will later become word-selective.

DISCUSSION

The human cerebral cortex contains dozens of functionally distinct regions, each arising in approximately the same location in almost every normal adult. How does this intricate and systematic organization arise in development? Here we test the hypothesis that the functional fate of a given cortical region may be determined by its earlier-developing pattern of connections with the rest of the brain, i.e. its "connectivity fingerprint". Consistent with this hypothesis, we find that the functional selectivity of VWFA arises between age 5 and age 8, when children learn to read, and that its cortical location at age 8 can be predicted by the distinctive connectivity of the same region at age 5, before the child can read and before the region differs functionally from nearby more general shape-responsive cortex.

The ability to predict the spatial pattern of word selectivity across the ventral pathway from earlier-developing voxelwise patterns of connectivity is robust, accounting for 69% of the reliable variance in word selectivity across voxels. Further, these predictions account for individual differences in the precise location of the VWFA, as the location of each 8-year-old's VWFA is better predicted by that child's own connectivity data at age 5 than it is by another child's connectivity pattern at age 5, or even by a group analysis of word selectivity in all the other children at age 8. Finally, we find no evidence that functional response profiles at age 5 can predict word selectivity at age 8. In particular, our finding that the

region that becomes the VWFA does not respond differentially to faces vs. letters before children learn to read argues against prior hypotheses that the region that becomes the VWFA starts out with a selectivity for letter-like features[16–18] or faces[19]. Taken together, these findings powerfully support the idea that earlier-developing patterns of connectivity instruct the development of cortical regions into functionally distinct regions.

The evidence presented here for an instructive role of connectivity in cortical development dovetails with the classic studies of "rewired" ferrets. In those studies, the cortical region that would otherwise have developed into primary auditory cortex instead took on many of the distinctive functional signatures of primary visual cortex after retinal input was rerouted (via MGN) to that location[5,6,7,8,9]). The current study extends the principle from primary sensory regions in ferrets to high-level cortical regions in humans.

Myriad questions remain for future research. First, while we found no evidence for a distinctive functional response at age 5 in the region that would later become the VWFA, this finding should be more extensively tested with a broader range of stimuli. One prior study[25] reported symbol selectivity in a nearby location in four year olds, but because that study used a cross sectional design it is possible that the region showing symbol selectivity at age four is different from the region that became the VWFA. Of particular interest is whether this region shows selectivity for foveal versus peripheral inputs, rectilinear versus curvilinear features, or any other feature bias that may predispose this region to become selective for visually presented words and letters.

A second important question is whether early connectivity also instructs functional development of other functionally distinctive extrastriate regions. This question will be difficult to answer given the great challenges of scanning children younger than 5 years of age, when face-selective regions are already evident in our data (but see [25], which finds no evidence of face-selectivity in the left fusiform in 4-year-olds). Pending such studies, it remains possible that the developmental mechanisms that give rise to the VWFA may differ from those for other cortical regions whose selectivity may be less dependent on experience.

Third, although the strong cross-lagged correlations we found within individuals are suggestive of a causal role of connectivity in determining later function, a direct causal test has yet to be run. Such a test may be possible in future by testing humans who sustained early disruptions of the relevant white matter connections e.g. from stroke. Our results accord with previous correlational studies showing that white matter bundles predict future reading ability in children who cannot read yet (and may indicate a structural basis of behavioral risk for dyslexia that predates reading instruction[26,27]). Future studies can investigate how pre-reading connectivity constrains future reading ability in individual subjects, and what aspects of this connectivity are malleable by early experience.

Finally, showing that distinctive connectivity arises before distinctive function begs the further question of how the connectivity fingerprint itself arose. Possible mechanisms that may determine patterns of connectivity, or that may work in tandem with connectivity to determine function, include molecular markers or tissue/circuit properties inherent in each cortical region (e.g. cytoarchitecture[28,29]). A combination of work on animal models, as well

as longitudinal studies and experiments of nature in humans, should be able to resolve these questions, providing a rich new picture of the mechanisms underlying the development of the human cortex.

In sum, our longitudinal, cross-lagged study supports the hypothesis that early connectivity instructs the functional development of the VWFA, a cortical region underlying the uniquely human ability to read. Further, the ability to predict later brain function from an anatomical scan that can be performed even in a sleeping infant may offer powerful new strategies for understanding and diagnosing neurodevelopmental disorders such as dyslexia and autism.

ONLINE METHODS

Participants

As part of a larger study, children completed a short battery of psychoeducational assessments in their schools in New England in the spring of pre-kindergarten or fall of kindergarten, before formal word reading instruction. A subset of children who completed screening were invited to participate in the brain imaging study. This study was approved by the institutional review boards at the Massachusetts Institute of Technology and Boston Children's Hospital. Parents gave written consent and children gave verbal assent to participate.

We collected DWI data and/or fMRI data from 112 children in pre-k or kindergarten ("Age 5" group). Three years later, we invited all children back to participate in another MRI study (which included both DWI and fMRI) after they completed 2nd grade ("Age 8" group). 33 children agreed to return and were scanned after completing 2nd grade; two individuals were excluded either for poor scan quality or for withdrawing from the study at the time of the scan. 20 of these children (pre-readers) were unable to read more than 5 high-frequency short words (WRMT-R/NU Word ID subtest[30]) when tested at age 5. We focused our analyses on these children because they could not read at the time of their pre-kindergarten scan.

9/20 children were excluded from longitudinal predictions analysis (6 did not have a kindergarten DWI scan; 3 had excessive DWI motion as determined by visual inspection; see Supplementary Materials for DWI and fMRI motion measures). Therefore, the longitudinal fMRI analysis included 14 children (4 females/11 males, 5.4 ± 0.09 years old at first scan, and 8.3 ± 0.07 years old at second scan) and the longitudinal DWI prediction analysis included 11 children (5 females/6 males, 5.5 ± 0.08 years at first scan, and 8.4 ± 0.05 years at second scan). All children met eligibility criteria including: being a native speaker of American English; born after at least 36 weeks gestation; no sensory or perceptual difficulties other than corrected vision; no history of head or brain injury or trauma; no neurological, neuropsychological, or developmental diagnoses; no medications affecting the nervous system; standard scores > 80 on measures of nonverbal IQ and vocabulary at age 5 (Kaufman Brief Intelligence Test [KBIT-2] Matrices[31]; Peabody Picture Vocabulary Test [PPVT-4][32]).

Structural image acquisition and processing

Structural, DWI, and fMRI data for both timepoints were acquired on a 3T Siemens Trio Tim MRI scanner with a standard Siemens 32-channel phased array head coil. A whole-head, high-resolution T1-weighted multiecho MPRAGE[33] anatomical volume was acquired at each timepoint (acquisition parameters: TR = 2350 ms, TE = 1.64 ms, TI = 1400 ms, flip angle = 7°, FOV = 192 × 192, 176 slices, voxel resolution = 1.0 mm^3, acceleration = 4). An online prospective motion correction algorithm reduced the effect of motion artifacts during the structural scan, and 10 selective reacquistion images were acquired and included to replace images that were affected by head motion[34].

Structural MRI data were processed using a semiautomated processing stream using the default parameters in FreeSurfer v5.2.0[35,36,37,38]; http://surfer.nmr.mgh.harvard.edu/), which includes motion and intensity correction, surface coregistration, spatial smoothing, subcortical segmentation, and cortical parcellation based on spherical template registration. The resulting cortical parcellation and subcortical segmentations were individually edited and reviewed for quality control and were used as seeds and targets for DWI tractography (below).

fMRI protocols

Age 5—Children viewed 2 runs of 20s blocks of black and white photographs of neutral expression faces, white letters, white false font stimuli, and a fixation condition (a total of 6 blocks per stimulus type). Stimuli were 800 × 800px and presented on a black background. False font stimuli were generated by rearranging parts of the same real letters and following orthographic patterns of English letters (e.g., no letter had ascending and descending aspects; Supplementary Figure 2). Stimuli were presented for 1500ms followed by a fixation cross for 500ms, for a total duration of 2000ms. Each run lasted 4 min 8s and consisted of 3 blocks each of letters, faces, false font letters, and fixation. Participants performed a one-back task, responding with a button-press to any image presented twice in a row (see Supplementary Table 1 for accuracies.

Age 8—Children viewed 6 runs of 18s blocks (26 stimuli+2 repetitions/block) of black and white line-drawings of faces, objects, words, scrambled words, and a fixation condition (Supplementary Figure 1). Line drawings were 300×300px, and words were of height 120px with width determined by the length of the word (minimum 120px and maximum 300px). A gray square grid with spacing 30px by 30px was placed over all images to best equate the different stimulus categories to the scrambled stimuli. To create the scrambled stimuli, the square sections of the gridded image were randomized. All stimuli were overlaid on a single-color background that changed color every 500ms. Stimuli were presented for 500ms with an ISI of 192.3ms (692ms per trial). Each run consisted of 19 blocks (4 blocks per category and 3 fixation blocks per run) and participants performed a one-back task, responding with a button-press for any image presented twice in a row.

fMRI acquisition parameters

Age 5—Data were collected with 3×3×4mm resolution, 2s TR, 30ms TE, 90° flip, 172 TRs, 64×64 base resolution, 32 slices approximately parallel to AC/PC line to cover the entire

cortex. Prior to each scan, four images were acquired and discarded to allow longitudinal magnetization to reach equilibrium. PACE, an online prospective motion correction algorithm[39], was implemented to reduce the effect of motion artifacts.

Age 8—Data were collected with 2mm^3 resolution, 2s TR, 30ms TE, 90° flip, 172 TRs, 100×100 base resolution, 25 slices approximately parallel to the base of the temporal lobe to cover the entire inferior temporal cortex. We additionally collected a fieldmap for distortion correction every two runs with the same slice prescription as the fMRI sequence (25 slices, 2mm^3 resolution, 500ms TR, 55° flip, 100×100 base resolution).

fMRI analysis

Age 5 fMRI data were analyzed using Nipype (http://nipy.org/nipype/index.html;[40]. Images were motion corrected using MCFLIRT and high-pass temporal filtering (using a cutoff of 120s). Functional images were coregistered to anatomical space using bbregister. Statistical analyses were conducted in FSL. Age 8 fMRI data were analyzed with Freesurfer (www.surfer.nmr.mgh.harvard.edu/), FsFast (www.surfer.nmr.mgh.harvard.edu/FsFast/), and custom Matlab code. Images were motion corrected (time points where the difference in total vector motion from the previous time point exceeded 1mm were excluded, and orthogonalized motion measures were used as nuisance regressors for the GLM), detrended, and fit using a standard gamma function (d = 2.25 and t = 1.25). Age 8 data were also distortion-corrected using the fieldmaps every two runs.

fROI definition

We used a watershed GSS method[41,42] to define a VWFA parcel as a search-space for the VWFA fROIs, from a separate group of adults who participated in exactly the same fMRI experiment. These parcels were registered to each child's native brain anatomy at age 8 using the inverse transform of Freesurfer's CVS toolbox[43,44]; https://surfer.nmr.mgh.harvard.edu/fswiki/mri_cvs_register) to the CVS average-35 template. Each child's contrast map for the even-runs was thresholded at P<0.005. Individual-subject fROIs were constructed from the intersection of the relevant parcel (for lFFA, VWFA, and lPFS separately) and the contrast map for the even runs (thresholded and not spatially-smoothed). Contrast maps for line-drawings of Faces > line-drawings of Objects defined lFFA, Words > Object line-drawings defined VWFA, and Object line-drawings > Scrambled words defined lPFS. These fROIs did not overlap in 7/14 children and had minimal overlap in the remaining children (2.84 ± 0.83% of the lFFA and VWFA fROIs overlapped and 2.87 ± 0.36% of the lFFA, VWFA, and lPFS overlapped). We removed any overlapping voxels between these fROIs, thus creating non-overlapping VWFA, lFFA, and lPFS fROIs in each individual's native anatomy. We used these non-overlapping fROIs for all further analyses. The odd runs (also not spatially smoothed) were then used for calculating percent signal change (PSC) for each stimulus category.

Motion measures

Total vector motion and root mean squared rotation were calculated using FSFast. Time-points that had more than 1mm total vector motion from the previous time-point were removed. We chose the best four runs of fMRI data for each subject as those with the fewest

time-points removed. After removing time-points for the best four runs, we averaged the measures of motion across runs for each subject. We also extracted motion measures from DWI data using TRACULA software[45]: average translation, rotation, percentage bad slices, and average drop-out score (for slices with excessive intensity drop-out).

We found that none of the fMRI motion measures was correlated with any of the DWI motion measures (at $p<0.05$; Supplementary Table 2).

Longitudinal registration of age 5 to age 8 data

We registered the age 5 anatomical data of each subject to the same subject's age 8 anatomical data using Advanced Normalization Tools (ANTs version 2.1.0; http://stnava.github.io/ANTs/) registration,[46,47]. ANTs has been previously used for lifespan analyses of brain morphology[48] and function[49] in both adult[48] and pediatric brain data[49,50,51] including infants[52]. We transformed the age 8 brain to the age 5 brain using the symmetric normalization toolbox with Gaussian regularization and initialized the transform with the affine registration matrix from Freesurfer's mri_robust_register software[53,54,55]; https://surfer.nmr.mgh.harvard.edu/fswiki/mri_robust_register).

We calculated the accuracy of the ANTs longitudinal registration for two structures: the large VWFA parcel, which we used as a search space to define the VWFA fROI for each subject, and the left occipitotemporal cortex region (lOTC, which is derived from combining the left fusiform and left inferior temporal gyrus from the Freesurfer parcellation; this region is important because we used it as a seed for tractography, explained below). We mapped either the VWFA parcel or the lOTC from age 8 to the age 5 anatomy using ANTs and calculated the overlap between this ANTs-registered region with the region defined by direct registration to the age 5 data (i.e. age 8 to age 5 -registered region vs. region registered directly to age 5). This procedure quantified error due to longitudinal registration. We used two measures of accuracy: the overlap coefficient and modified Hausdorff. The overlap coefficient is the size of the intersection of the two regions divided by the minimum size of the two regions. The modified Hausdorff[45] is defined as the minimum distance of each voxel in one region from the other region, averaged over all voxels in the two regions (i.e. average distance from the age 8-to-age 5 registered region to the native age 5 region); this measure indicates that all points in the registered region are on average "X" far from the native age 5 region. The overlap coefficient for the lOTC was 0.8700 ± 0.0063 and 0.8731 ± 0.0084 for the VWFA parcel; the modified Hausdorff metric was 0.1471 ± 0.0133 voxels for the lOTC anatomical region, and 0.1437 ± 0.0142 voxels for the VWFA parcel.

Comparison of the VWFA's selectivity to letters and words

The fMRI data at age 5 had slightly different stimulus conditions than the fMRI data acquired at age 8: age 5 data included letters instead of words and did not include an "Objects" condition. To test whether the VWFA responds selectively not only to words but also to individual letters, we performed several experiments in a cohort of adults: the VWFA localizer i.e. "age 8 fMRI experiment", and a version of the VWFA localizer that included individual letters in addition to the other 4 categories (line-drawings of objects, line-drawings of faces, words, and scrambled words). The VWFA localizer (i.e. age 8 fMRI

experiment) was collected in another scan session and we used that scan session to define the VWFA, lFFA, and lPFS in exactly the same way that we defined them for children. We compared letter vs. word selectivity in each of these regions. We compared VWFA letter-selectivity and word-selectivity vs. selectivities to the other categories in adults. The VWFA showed a significant interaction by condition (repeated measures ANOVA by condition: F_4 = 22.26, P = 1.76 $\times 10^{-5}$). The response to letters and words in the VWFA did not differ significantly (T = 0.16, P = 0.885) and each of these conditions produced a significantly higher response than the object condition (letters vs. objects: T = 5.66, P = 1.09 $\times 10^{-2}$; words vs. objects: T = 9.27, P = 2.66 $\times 10^{-3}$). The lFFA and lPFS showed higher responses to faces and objects, respectively, over any other category, including words and letters (lFFA: ANOVA interaction: F_4 = 31.86, P = 2.63 $\times 10^{-6}$; faces vs. words, letters: T = 4.20, P = 2.46 $\times 10^{-2}$; T = 8.10, P = 3.93 $\times 10^{-3}$; lPFS: F_4 = 11.50, P = 4.53 $\times 10^{-4}$; objects vs. words, letters: T = 3.76, P = 3.30 $\times 10^{-2}$; T = 3.60, P = 3.68 $\times 10^{-2}$). These analyses confirm that the VWFA shows no difference in the response to words vs. individual letters, with both conditions significantly higher than to objects. Thus, if the VWFA was selective to orthography at age 5, we would have expected to find comparable selectivity to letters at age 5 as we observed for words at age 8.

DWI image acquisition

The diffusion-weighted scan in kindergarten (5 min total) included 10 non-diffusion weighted volumes (b = 0) and 30 diffusion-weighted volumes (i.e. 30 diffusion directions) acquired with non-colinear gradient directions (b = 700 s/mm^2), all at 128 × 128 base resolution and isotropic voxel resolution of 2.0 mm^3. Diffusion weighted images were checked for motion artifact and processed using FSL's FDT software (http://www.fmrib.ox.ac.uk/fsl/fdt/index.html[56].

The diffusion-weighted scan at age 8 was identical to the kindergarten scan except that it included 60 diffusion-weighted volumes (b = 700 s/mm^2) because the children could stay motionless in the scanner for longer periods of time. Children watched a movie of their choice during the anatomical and DWI scanning.

DWI longitudinal prediction analysis

We registered the age 5 Freesurfer segmentation and parcellation results (aparc+aseg) to each individual's age 5 diffusion images using Freesurfer's bbregister function[57], which uses surface-based algorithms to register images, and we initialized the registration with FSL's FLIRT. We combined the DWI-registered left fusiform and left inferior temporal gyrus parcels into one seed region (left occipitotemporal seed region; lOTC). Each voxel within this region was used as a seed and the remaining 81 parcels were used as target regions for fiber tracking. The principal diffusion directions were calculated per voxel, and probabilistic diffusion tractography was carried out using FSL-FDT[56] with 10,000 streamline samples in each seed voxel to create a connectivity distribution to each of the target regions, while avoiding a mask consisting of the ventricles. Thus, every voxel within the lOTC seed region was described by a vector of connection probabilities to each other brain region.

Each participant's age 8 functional image (t-statistic) for the contrast of Words > Objects from either the best 4 runs (assessed by least motion; see Supplementary Materials) or even runs (for split-half reliability measurements) was registered to his or her structural image at age 5 using the **Longitudinal Registration** approach described above, and the resulting registered functional image was then registered to the age 5 DWI data using Freesurfer's bbregister and initialized using FSL's FLIRT. Thus, every voxel was also described by a vector of t-statistics for each functional contrast.

To predict function from connectivity, we used the methods described in [1] and [2]. Briefly, we used a leave-one-subject-out cross-validation (LOOCV) routine[58], where a single subject's data was excluded, trained a model with all of the remaining subjects' voxelwise data, and then applied the model to the left-out subject. This routine was repeated for all subjects, generating independent predictions. Each voxel of the seed parcel was paired with its connectivity vector to every other brain region, its spatial coordinates, and its word-selectivity (response to Words > Objects). We used in-house MATLAB code (R2011b; The Mathworks, Natick, MA) and the LibSVM toolbox (http://www.csie.ntu.edu.tw/~cjlin/libsvm/) for these analyses. We concatenated all of the native-space voxels from each subject's lOTC seed region (excluding all voxels of the left-out subject) and trained an SVR model with kernel=radial basis function, γ = 0.012 (1/number of features), ε = 0.1) on the standardized and linearized word-selectivity and connectivity vector of that voxel. Thus each voxel was an independent observation in the regression model. Because all analyses were performed on subject-specific anatomy, the number of voxels in the seed varied among individuals, but the model was blind to the participant each voxel belonged to. We applied this model to the DWI data of the subject that we left out of the analysis, resulting in a predicted fMRI value for word-selectivity for every voxel of the lOTC seed region. To evaluate the accuracy of the predictions, we performed Pearson's correlations on the predicted vs. actual fMRI responses for each individual and Fisher z-transformed the resulting correlation coefficients. These prediction accuracies were tested against random permutations and other benchmarks (below).

Random permutations

We used the same data matrices that were used for DWI predictions but here we shuffled the pairings between the fMRI responses and DWI connectivity vectors. We shuffled these 5000 times, generating 5000 predictions from randomly shuffled data for each subject, and performed a permutation test (exact test) of each subject's z-transformed correlation coefficient for DWI predictions against the distribution of correlation coefficients from the permutations.

Group-average prediction analysis

We compared the accuracy of the DWI predictions with a group analysis model (see [1,2]). The group models were also made through LOOCV. Each participant's functional data at age 8 were spatially normalized into CVS average 35 template space with Freesurfer's CVS registration and superimposed to create composite maps. We performed a least squares random-effects test on all but one participant using Freesurfer's FsFast. The resulting t-statistic image, which was based on all the other participants in normalized CVS space, was

then mapped to the native age 5 anatomy of the participant left out of the group analysis (using the reverse CVS normalization transform from age 5 to group template space). We again correlated the actual vs. predicted fMRI values within the lOTC seed mask, Fisher z-transformed the resulting coefficients, and performed a paired t-test to compare DWI prediction accuracies to group prediction accuracies.

Subject–to–subject prediction analysis

We mapped each child's anatomical data at age 8 to each other child's anatomical data at age 5 using ANTS software (see **Longitudinal Registration** section). We used Freesurfer's bbregister function to map the fMRI data at age 8 to the anatomical data at age 8, and then mapped the registered fMRI data to every other child's anatomy (using the registration matrix from ANTS software). We then registered that data to the DWI data using bbregister. This process of registering each child's fMRI data at age 8 to each other child's DWI data at age 5 generated voxelwise predictions for each subject based on each other's child's data.

Split-half reliability

We also compared the DWI predictions to "ceiling predictions" or predictions of age 8 word-selectivity from left-out age 8 fMRI runs. We divided the residual sum of squares for the DWI predictions by the total sum of squares for the split-half reliability to calculate the normalized (R^2). This measurement represents the best possible predictions of functional selectivity for each subject because they are based on the same subject's own fMRI data. It also captures the reliability of the fMRI data, and can therefore be used to normalize the DWI prediction accuracies and assess how much of the reliable variance (R^2) in age 8 word-selectivity can be predicted from age 5 DWI data.

Overlap measurements

We generated an fROI from the DWI predictions by masking the DWI predicted fMRI responses with the larger VWFA GSS parcel (see **fROI definition** section) and thresholded the DWI predictions at > 0.4 s.u. (same threshold as Figure 3) as well as upper bound (>0.8 s.u.) and lower bound (>0.2 s.u.). We generated the actual fROIs using the same criteria. We also generated fROIs from the split-half fMRI data in exactly the same manner. We compared the DWI predicted fROIs (and the split-half predicted fROIs) to the actual fROIs for each subject using the same two measures as the **Longitudinal Registration** section (overlap coefficient and modified Hausdorff metric).

fROI-based DWI tractography analysis

The VWFA, lFFA, and lPFS were used as seed regions for fiber tracking for each individual; the remaining 81 individual-subject parcels from the Freesurfer segmentation were similarly DWI-registered, and used as the target regions for tractography (we excluded the fusiform and inferior temporal gyrus as targets because the voxels within VWFA, lFFA, and/or lPFS landed somewhere within these regions and it would be redundant to include a region as both a seed and a target). Tractography was run from each seed fROI to each target parcel (and back) and averaged the connectivity values to and from the fROIs. We performed a 2-way ANOVA to compare lFFA, VWFA, and lPFS connectivity to the 81 target regions. We

also performed separate 2-way ANOVAs to compare the VWFA to the lFFA and lPFS separately, and post-hoc t-tests were performed if we observed a significant fROI × target interaction.

Statistics

We used a within-subject design in these experiments; therefore, there was no experimental group randomization or blinding. We followed standard procedures in the field and statistical procedures in line with previously published studies[1,257]. All Student's T-tests are paired and two-tailed; F-tests in ANOVAs and exact permutation tests were one-tailed, as is standard for such comparisons. Data distribution was assumed to be normal, but this was not formally tested. No statistical methods were used to pre-determine sample sizes but our sample sizes are similar to those reported in previously published longitudinal studies in children or fMRI studies on decoding and prediction within subject (e.g. [59,60]).

Data availability

The data that support the findings of this study are available from the corresponding author upon request.

Supplementary Material

Refer to Web version on PubMed Central for supplementary material.

Acknowledgments

NICHD/NIH grant F32HD079169 to ZS, NIH/NICHD R01HD067312 to JDEG and NG, Ellison Medical Foundation, EY13455 to NK, Grant 1444913 from McGovern Institute for Brain Research MINT to NK and ZS

We thank B.Fischl and M.Reuter for their guidance and advice on longitudinal registration, S. Robinson and O. Ozernov-Palchik for assistance with participant coordination and A. Park for technical assistance. We thank the Athinoula A. Martinos Imaging Center at the McGovern Institute for Brain Research at MIT and its staff. We also thank our READ Study research testers, school coordinators and principals, and participating families.

REFERENCES

1. Saygin ZM, et al. Anatomical connectivity patterns predict face selectivity in the fusiform gyrus. Nat. Neurosci. 2012; 15:321–327. [PubMed: 22197830]
2. Osher DE, et al. Structural Connectivity Fingerprints Predict Cortical Selectivity for Multiple Visual Categories across Cortex. Cereb. Cortex. 2015 bhu303.
3. Mahon BZ, Caramazza A. What drives the organization of object knowledge in the brain? Trends Cogn. Sci. 2011; 15:97–103. [PubMed: 21317022]
4. Hannagan T, Amedi A, Cohen L, Dehaene-Lambertz G, Dehaene S. Origins of the specialization for letters and numbers in ventral occipitotemporal cortex. Trends Cogn. Sci. 2015; 19:374–382. [PubMed: 26072689]
5. Sur M, Garraghty PE, Roe AW. Experimentally induced visual projections into auditory thalamus and cortex. Science. 1988; 242:1437–1441. [PubMed: 2462279]
6. Roe AW, Pallas SL, Hahm JO, Sur M. A map of visual space induced in primary auditory cortex. Science. 1990; 250:818–820. [PubMed: 2237432]
7. Roe AW, Pallas SL, Kwon YH, Sur M. Visual projections routed to the auditory pathway in ferrets: receptive fields of visual neurons in primary auditory cortex. J. Neurosci. 1992; 12:3651–3664. [PubMed: 1527604]

8. Sharma J, Angelucci A, Sur M. Induction of visual orientation modules in auditory cortex. Nature. 2000; 404:841–847. [PubMed: 10786784]
9. Horng S, et al. Differential Gene Expression in the Developing Lateral Geniculate Nucleus and Medial Geniculate Nucleus Reveals Novel Roles for Zic4 and Foxp2 in Visual and Auditory Pathway Development. J. Neurosci. 2009; 29:13672–13683. [PubMed: 19864579]
10. McCandliss BD, Cohen L, Dehaene S. The visual word form area: expertise for reading in the fusiform gyrus. Trends Cogn. Sci. 2003; 7:293–299. [PubMed: 12860187]
11. Dehaene S, et al. How Learning to Read Changes the Cortical Networks for Vision and Language. Science. 2010; 330:1359–1364. [PubMed: 21071632]
12. Glezer LS, Jiang X, Riesenhuber M. Evidence for highly selective neuronal tuning to whole words in the 'Visual Word Form Area'. Neuron. 2009; 62:199–204. [PubMed: 19409265]
13. Glezer LS, Riesenhuber M. Individual Variability in Location Impacts Orthographic Selectivity in the 'Visual Word Form Area'. J. Neurosci. 2013; 33:11221–11226. [PubMed: 23825425]
14. Glezer LS, Kim J, Rule J, Jiang X, Riesenhuber M. Adding Words to the Brain's Visual Dictionary: Novel Word Learning Selectively Sharpens Orthographic Representations in the VWFA. J. Neurosci. 2015; 35:4965–4972. [PubMed: 25810526]
15. Baker CI, et al. Visual word processing and experiential origins of functional selectivity in human extrastriate cortex. Proc. Natl. Acad. Sci. U. S. A. 2007; 104:9087–9092. [PubMed: 17502592]
16. Srihasam K, Vincent JL, Livingstone MS. Novel domain formation reveals proto-architecture in inferotemporal cortex. Nat. Neurosci. 2014; 17:1776–1783. [PubMed: 25362472]
17. Grill-Spector K, Kourtzi Z, Kanwisher N. The lateral occipital complex and its role in object recognition. Vision Res. 2001; 41:1409–1422. [PubMed: 11322983]
18. Dehaene S, Cohen L. Cultural Recycling of Cortical Maps. Neuron. 2007; 56:384–398. [PubMed: 17964253]
19. Dehaene S, Cohen L. The unique role of the visual word form area in reading. Trends Cogn. Sci. 2011; 15:254–262. [PubMed: 21592844]
20. Haxby JV, et al. Distributed and Overlapping Representations of Faces and Objects in Ventral Temporal Cortex. Science. 2001; 293:2425–2430. [PubMed: 11577229]
21. Behrmann M, Plaut DC. Distributed circuits, not circumscribed centers, mediate visual recognition. Trends Cogn. Sci. 2013; 17:210–219. [PubMed: 23608364]
22. Tavor I, et al. Task-free MRI predicts individual differences in brain activity during task performance. Science. 2016; 352:216–220. [PubMed: 27124457]
23. Bouhali F, et al. Anatomical Connections of the Visual Word Form Area. J. Neurosci. 2014; 34:15402–15414. [PubMed: 25392507]
24. Yeatman JD, Rauschecker AM, Wandell BA. Anatomy of the visual word form area: adjacent cortical circuits and long-range white matter connections. Brain Lang. 2013; 125:146–155. [PubMed: 22632810]
25. Cantlon JF, Pinel P, Dehaene S, Pelphrey KA. Cortical Representations of Symbols, Objects, and Faces Are Pruned Back during Early Childhood. Cereb. Cortex. 2011; 21:191–199. [PubMed: 20457691]
26. Saygin ZM, et al. Tracking the Roots of Reading Ability: White Matter Volume and Integrity Correlate with Phonological Awareness in Prereading and Early-Reading Kindergarten Children. J. Neurosci. 2013; 33:13251–13258. [PubMed: 23946384]
27. Langer N, et al. White Matter Alterations in Infants at Risk for Developmental Dyslexia. Cereb. Cortex. 2015 bhv281.
28. Brodmann, K. Vergleichende Lokalisationslehre der Grosshirnrinde in ihren Prinzipien dargestellt auf Grund des Zellenbaues. Barth: 1909.
29. Lorenz S, et al. Two New Cytoarchitectonic Areas on the Human Mid-Fusiform Gyrus. Cereb. Cortex. 2015 bhv225.
30. Woodcock, RW. Woodcock Reading Mastery Tests, Revised, Examiner's Manual. American Guidance Service; 1998.
31. Kaufman, AS.; Kaufman, NL. Kaufman brief intelligence test. Wiley Online Library; 2004.
32. Dunn, DM.; Dunn, LM. Peabody picture vocabulary test: Manual. Pearson: 2007.

33. Van der Kouwe AJW, Benner T, Salat DH, Fischl B. Brain morphometry with multiecho MPRAGE. NeuroImage. 2008; 40:559–569. [PubMed: 18242102]
34. Tisdall MD, et al. Volumetric navigators for prospective motion correction and selective reacquisition in neuroanatomical MRI. Magn. Reson. Med. 2012; 68:389–399. [PubMed: 22213578]
35. Dale AM, Fischl B, Sereno MI. Cortical surface-based analysis. I. Segmentation and surface reconstruction. NeuroImage. 1999; 9:179–194. [PubMed: 9931268]
36. Fischl B, et al. Whole brain segmentation: automated labeling of neuroanatomical structures in the human brain. Neuron. 2002; 33:341–355. [PubMed: 11832223]
37. Fischl B, et al. Automatically parcellating the human cerebral cortex. Cereb. Cortex N. Y. N. 1991; 2004; 14:11–22.
38. Desikan RS, et al. An automated labeling system for subdividing the human cerebral cortex on MRI scans into gyral based regions of interest. NeuroImage. 2006; 31:968–980. [PubMed: 16530430]
39. Thesen S, Heid O, Mueller E, Schad LR. Prospective acquisition correction for head motion with image-based tracking for real-time fMRI. Magn. Reson. Med. 2000; 44:457–465. [PubMed: 10975899]
40. Gorgolewski K, et al. Nipype: a flexible, lightweight and extensible neuroimaging data processing framework in python. Front. Neuroinformatics. 2011; 5:13.
41. Fedorenko E, Hsieh P-J, Nieto-Castañón A, Whitfield-Gabrieli S, Kanwisher N. New Method for fMRI Investigations of Language: Defining ROIs Functionally in Individual Subjects. J. Neurophysiol. 2010; 104:1177–1194. [PubMed: 20410363]
42. Julian JB, Fedorenko E, Webster J, Kanwisher N. An algorithmic method for functionally defining regions of interest in the ventral visual pathway. NeuroImage. 2012; 60:2357–2364. [PubMed: 22398396]
43. Postelnicu G, Zollei L, Fischl B. Combined Volumetric and Surface Registration. IEEE Trans. Med. Imaging. 2009; 28:508–522. [PubMed: 19273000]
44. Zöllei L, Stevens A, Huber K, Kakunoori S, Fischl B. Improved Tractography Alignment Using Combined Volumetric and Surface Registration. NeuroImage. 2010; 51:206–213. [PubMed: 20153833]
45. Yendiki A, et al. Automated probabilistic reconstruction of white-matter pathways in health and disease using an atlas of the underlying anatomy. Front. Neuroinformatics. 2011; 5:23.
46. Wang H, Yushkevich PA. Multi-atlas segmentation with joint label fusion and corrective learning—an open source implementation. Front. Neuroinformatics. 2013; 7
47. Menze BH, et al. The Multimodal Brain Tumor Image Segmentation Benchmark (BRATS). IEEE Trans. Med. Imaging. 2015; 34:1993–2024. [PubMed: 25494501]
48. Tustison NJ, et al. Large-scale evaluation of ANTs and FreeSurfer cortical thickness measurements. NeuroImage. 2014; 99:166–179. [PubMed: 24879923]
49. Avants BB, et al. The Insight ToolKit image registration framework. Front. Neuroinformatics. 2014; 8:44.
50. Jain V, et al. Longitudinal reproducibility and accuracy of pseudo-continuous arterial spin-labeled perfusion MR imaging in typically developing children. Radiology. 2012; 263:527–536. [PubMed: 22517961]
51. Lawson GM, Duda JT, Avants BB, Wu J, Farah MJ. Associations between children's socioeconomic status and prefrontal cortical thickness. Dev. Sci. 2013; 16:641–652. [PubMed: 24033570]
52. Pineda RG, et al. Alterations in brain structure and neurodevelopmental outcome in preterm infants hospitalized in different neonatal intensive care unit environments. J. Pediatr. 2014; 164:52–60.e2. [PubMed: 24139564]
53. Reuter M, Rosas HD, Fischl B. Highly Accurate Inverse Consistent Registration: A Robust Approach. NeuroImage. 2010; 53:1181–1196. [PubMed: 20637289]
54. Reuter M, Fischl B. Avoiding asymmetry-induced bias in longitudinal image processing. Neuroimage. 2011; 57:19–21. [PubMed: 21376812]

55. Reuter M, Schmansky NJ, Rosas HD, Fischl B. Within-subject template estimation for unbiased longitudinal image analysis. Neuroimage. 2012; 61:1402–1418. [PubMed: 22430496]

56. Behrens TEJ, Berg HJ, Jbabdi S, Rushworth MFS, Woolrich MW. Probabilistic diffusion tractography with multiple fibre orientations: What can we gain? NeuroImage. 2007; 34:144–155. [PubMed: 17070705]

57. Greve DN, Fischl B. Accurate and robust brain image alignment using boundary-based registration. NeuroImage. 2009; 48:63–72. [PubMed: 19573611]

58. Hastie, T.; Tibshirani, R.; Friedman, J. The Elements of Statistical Learning: Data Mining, Inference, and Prediction. Springer: 2009.

59. Huth AG, de Heer WA, Griffiths TL, Theunissen FE, Gallant JL. Natural speech reveals the semantic maps that tile human cerebral cortex. Nature. 2016; 532:453–458. [PubMed: 27121839]

60. Finn AS, Sheridan MA, Kam CLH, Hinshaw S, D'Esposito M. Longitudinal Evidence for Functional Specialization of the Neural Circuit Supporting Working Memory in the Human Brain. J. Neurosci. 2010; 30:11062–11067. [PubMed: 20720113]

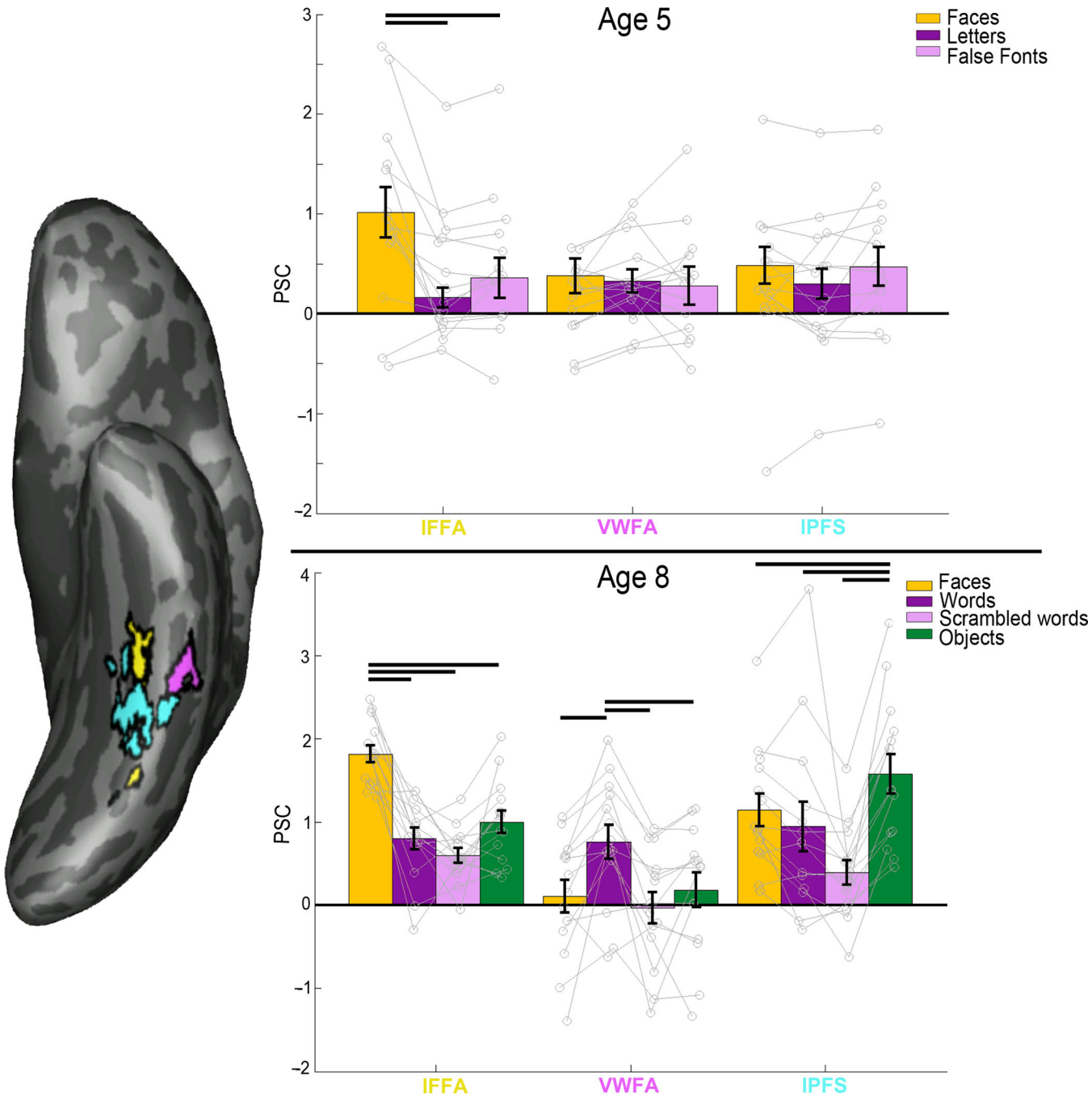

Figure 1.

Percent signal change (PSC) for each fROI. Left: inflated surface of an example subject, showing each of their fROIs defined from age 8 data (lFFA in yellow, VWFA in magenta, lPFS in cyan). Top: mean PSCs at age 5 in fROIs defined on age 8 data (registered to 5-year-old brain). Before a child is able to read, there is no selectivity to letters, letter-like stimuli (false fonts) or faces in the region that later becomes the VWFA, while lFFA shows clear selectivity for faces even at this age. Bottom: mean PSCs at age 8. We find clear selectivity for faces in lFFA and clear selectivity for words in the VWFA at age 8 in data not used to

define the fROI. Error bars denote standard error. Horizontal bars reflect significant post-hoc paired t-tests ($P < 0.05$, N=14).

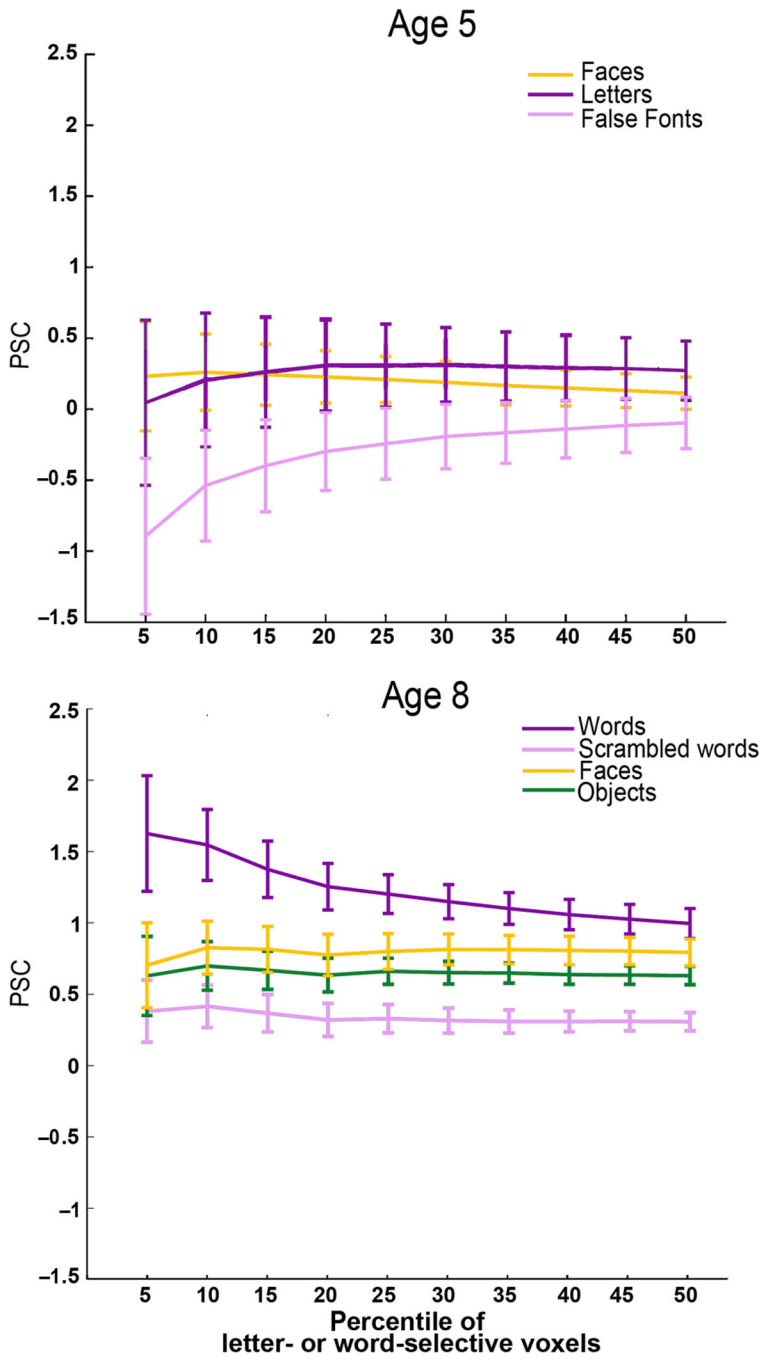

Figure 2.

Percent signal change in the VWFA as a function of fROI volume. To further test whether there was any selectivity for orthography at age 5, we performed a "binned" analysis where we used one run of age 5 data to define the Nth percentile of letter-selective voxels anywhere within the larger VWFA parcel (i.e. constraint region in Supplementary Figure 1 based on independent data in adults); we then measured the PSC to each condition in the other run of age 5 fMRI data in those same voxels. Children who were not able to read at age 5 did not show selectivity for letters as compared to faces or false fonts (top). The analogous analysis

of the age 8 data in the same children (bottom) found strong selectivity for words. Error bars reflect standard error of the mean for N = 14 subjects.

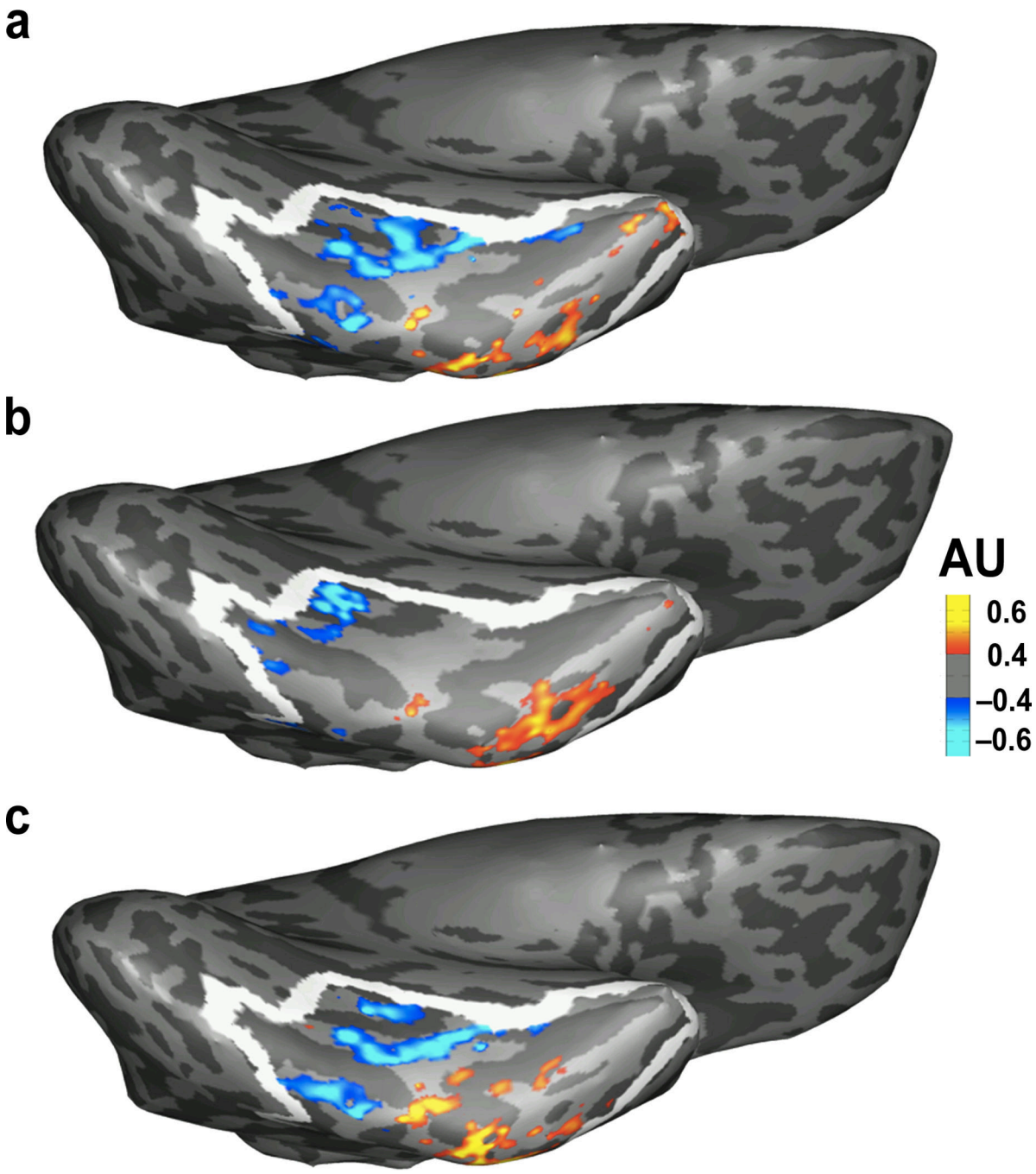

Figure 3.

Actual vs. predicted fMRI activation for Words > Objects on the ventral surface of an example subject. Heatmap reflects word selectivity and white outline indicates the boundaries of the left occipitotemporal anatomical parcel. AU = arbitrary units. (**a**) Actual fMRI activation for Words > Objects at age 8. (**b**) Activation that is predicted from the same individual's DWI data at age 5. (**c**) Activation that is predicted from the same individual's fMRI data at age 8, from independent, left-out fMRI runs from (**a**). This split-half reliability illustrates the best possible predictions that one could make about an individual's word

selectivity. The predicted activation from DWI matches the actual activation pattern, capturing loci that are accurately predicted from left-out data. Note that all images (actual, predicted from DWI, and predicted from left-out data) are based on (or trained on) an equal number of fMRI runs.

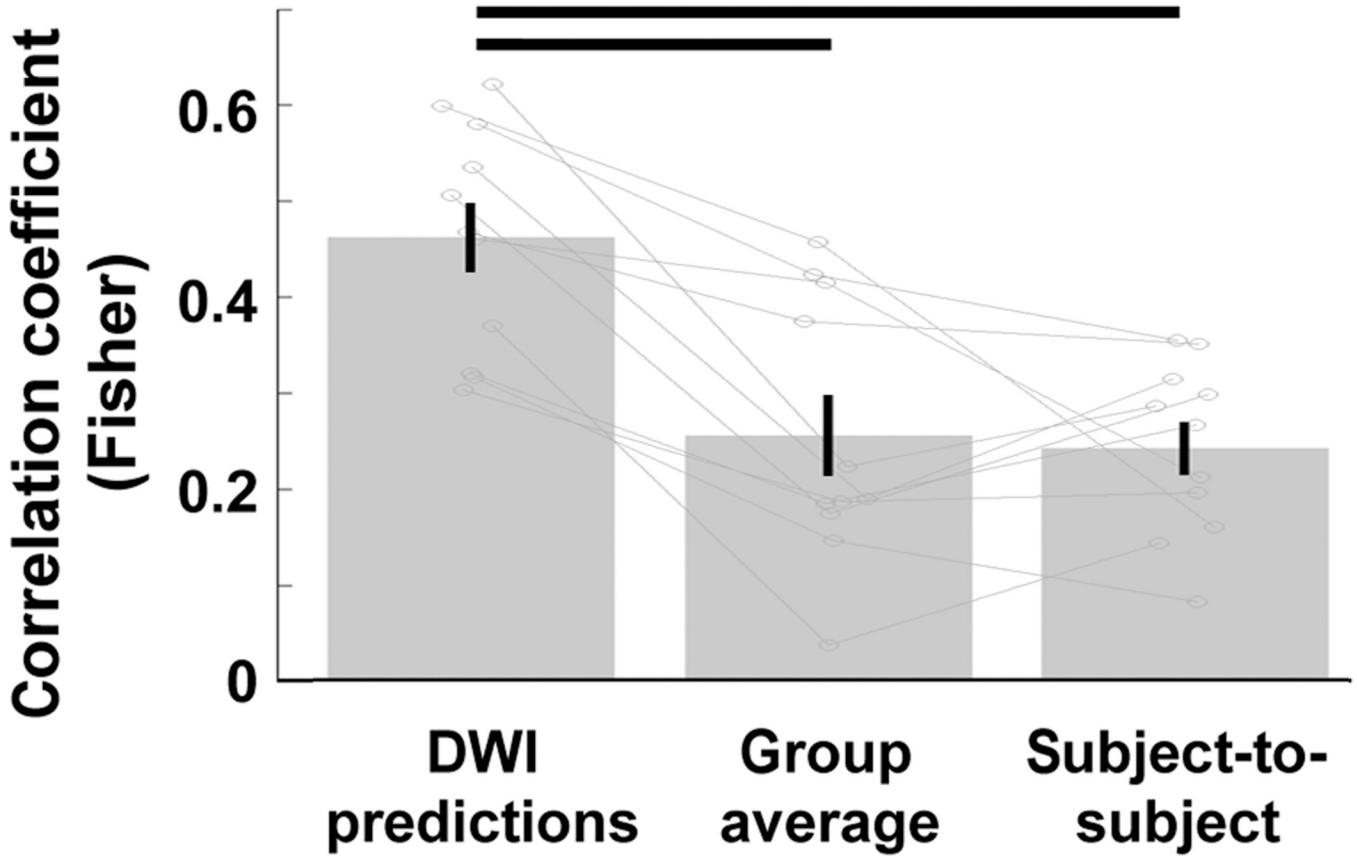

Figure 4.

Correlations of actual word-selectivity at age 8 with predicted word selectivity. Predictions of age 8 word-selectivity from age 5 DWI data were compared to predictions from the age 8 fMRI data of all other subjects (group average) and to predictions from each other subject's age 8 data. DWI predictions outperformed both of these types of predictions, demonstrating that the prediction of functional activation patterns from connectivity at age 5 is spatially precise enough to predict individual differences in functional activation patterns. Horizontal bars reflect significant differences (paired t-tests, each $P < 0.05 \times 10^{-4}$, N = 11); error bars reflect standard error of the mean.

Figure 5.

Left-lateralized regions that are preferentially connected with the VWFA vs. lFFA or lPFS at age 5. Color bar reflects T-values from the VWFA vs. lFFA comparison (post-hoc paired t-tests, $p < 0.05$). Connectivity (of the region that will become the VWFA) to these regions is already elevated (compared to nearby cortex) at age 5, even when no evidence of functional differentiation exists in the VWFA at that age.